

The Structure of the Mariana arc as inferred
AC .H3 no.S79 15471



Sager, William W.
SOEST Library

Solid earth

RETURN TO
HAWAII INSTITUTE OF GEOPHYSICS
LIBRARY ROOM **THESIS**

*070
Sag
str
ms*

STRUCTURE OF THE MARIANA ARC
AS INFERRED FROM
GRAVITY AND SEISMIC DATA

A THESIS SUBMITTED TO THE GRADUATE DIVISION OF THE
UNIVERSITY OF HAWAII IN PARTIAL FULFILLMENT
OF THE REQUIREMENTS FOR THE DEGREE OF

MASTER OF SCIENCE

IN GEOLOGY AND GEOPHYSICS

MAY 1979

By

William W. Sager

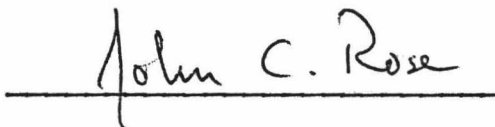
Thesis Committee:

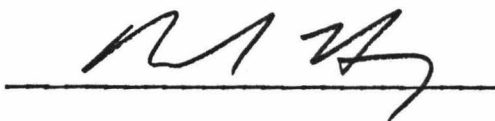
Donald M. Hussong, Chairman
John C. Rose
Richard N. Hey

We certify that we have read this thesis and that in our opinion it is satisfactory in scope and quality as a thesis for the degree of Master of Science in Geology and Geophysics.

THESIS COMMITTEE


Chairman


John C. Rose



ACKNOWLEDGEMENTS

This volume is dedicated to the memory of Dr. Stanley M. Sager, my father, who passed away January 11, 1979. A special thank you to Dr. D.M. Hussong for his suggestions and criticism. Suggestions from J.C. Rose and R.N. Hey were very helpful in preparing the manuscript.

This work was supported by International Phase of Ocean Drilling site survey grants CU-Hawaii 25903 and 25906.

ABSTRACT

A two dimensional gravity model of the lithosphere was constructed along a seismic refraction line, 800 km in length, across the Mariana arc near 18° N latitude. Included in the model are crustal layers constrained by seismic refraction results, an estimate of the gravity anomaly due to the subducting slab, and a model of the low density mantle beneath the Mariana Trough (an active, extensional, back-arc basin).

Several notable anomalies are found in the crustal layers. East of the trench, the crust is thinned slightly to account for an outer gravity high. Behind the landward wall of the trench, a small low density wedge is modeled. Also, an unusual configuration for the sub-arc root is required to fit the observed gravity anomaly.

The gravity anomaly due to the low density mantle in the trough is a -170 mgal negative centered approximately on the axial bathymetric high of the trough. Different depths to the bottom of the low density mantle are modeled. The best fits are obtained using depths between 100-400 km with corresponding density anomalies between -0.057 to -0.024 g/cc (relative to 3.35 g/cc). The anomaly associated with the low density mantle is concentrated in the center of the trough by assuming the lithosphere to thicken with distance away from the axial high.

TABLE OF CONTENTS

ACKNOWLEDGEMENTS	iii
ABSTRACT.....	iv
LIST OF TABLES.....	vi
LIST OF ILLUSTRATIONS.....	vii
INTRODUCTION.....	1
THE MARIANA ARC.....	2
DATA.....	4
THE MODEL.....	6
The crustal layers.....	6
The downgoing slab.....	7
The Low Density Mantle.....	9
DISCUSSION.....	14
CONCLUSIONS.....	18
APPENDIX: . LOW DENSITY MANTLE ANOMALIES CALCULATED FROM BACK ARC THERMAL MODELS.....	19
BIBLIOGRAPHY.....	42

LIST OF TABLES

Table	Page
1 Densities and depths used in the low density mantle models.....	13

LIST OF ILLUSTRATIONS

Figure		Page
1	Map of the Study Area.....	23
2	The observed and calculated Gravity Anomalies and the Crustal Model.....	25
3	The Downgoing Slab Model.....	27
4	The Low Density Mantle Model.....	29
5	Gravity Anomalies From Major Bodies in the Model.....	31
6	Low Density Mantle Gravity Anomalies....	33
A1	The Density Model Derived From Andrews and Sleep (1974).....	35
A2	The Density Model Derived from Schubert et al. (1975).....	37
A3	The Density Model Derived From Sydora et al. (1978).....	39
A4	A Comparison of the Calculated Anomaly over the Mariana Trough Using Several Different Thermal Models.....	41

INTRODUCTION

The gravitational signatures of island arc complexes have been of considerable interest to geophysicists during the last two decades. The first gravity models of trench arc systems tended to emphasize the role of crustal structures. Often any structure deeper than the Moho was ignored (Talwani et al., 1959b, 1961). As seismology offered compelling evidence for deeper structure in the form of Benioff zone earthquakes (Isacks et al., 1968), investigators modeled the gravity effect of the subducting slab (Hatherton, 1969, 1970, Oxburgh and Turcotte, 1970). The complexity of the slab models has increased in recent years (Grow, 1973, Toksoz et al., 1973, Grow and Bowin, 1975).

The crust of the marginal sea is thin and shallow, and thus the mantle is near the surface. This situation should lead to a large positive gravity anomaly over the basin. However, it has been noted that the gravity anomalies associated with actively extensional back-arc basins are smaller than expected (Talwani et al., 1961). Even so, few investigators have attempted to model the anomalously low density mantle which apparently causes the discrepancy. These models are notable in their diversity. Much of the difference is due to the lack of constraining data on the back-arc mantle. In light of plate tectonics most of these models are unreasonable or incomplete. The model in this study was constructed with both the current knowledge of island arcs and the good and bad points of these models in mind.

Perhaps the most critical parameter of any study of the mantle is the thermal field within that layer. Certainly, the thermal state of the mantle will greatly affect its density. Thus in this study it is necessary to consider the current knowledge of the thermal regime of the mantle.

Quite a number of authors have modeled the thermal

field of the subducting slab (McKenzie, 1970, Oxburgh and Turcotte, 1970, Minear and Toksoz, 1970, Toksoz et al., 1971, 1973, Griggs, 1972, Turcotte and Schubert, 1973, Schubert et al., 1975). These models may be distinguished by the extent to which they account for heating of the slab due to radioactivity, thermal conduction, friction, adiabatic compression, phase changes, and the angle and rate of descent of the slab. Despite their differences, the various models have produced very similar results (e.g. Anderson et al., 1976, Figure 2, Delany and Helgeson, 1978, Figure 15).

A few investigators have attempted to model the temperatures in the mantle above the slab (McKenzie, 1970, Hasebe et al., 1970, Andrews and Sleep, 1974, Schubert et al., 1975, Toksoz and Bird, 1977, Sydora et al., 1978). These models translate the mantle isotherms upward by either calling upon the diapiric rise of heated magma from the Benioff zone or convection in the mantle due to the drag of the downgoing slab. The results are not very similar, but it is unclear whether this is due to a fundamental difference in the mechanisms involved or just differences in the initial assumptions of the models.

The Mariana Arc

The Mariana arc marks the site of the Pacific plate's plunge beneath the Phillipine plate. Nearly a score of active volcanic islands, composed largely of basaltic andesite (Karig, 1971a), comprise the Mariana arc. Convex towards the east, the arc stretches from 12N to 25N at approximately 145E, as shown in Figure 1.

The Mariana trench connects the Bonin trench, on the north, with the Yap trench, to the south. Estimates of the rate of subduction vary widely. A median estimate, approximately 90 mm/yr (Toksoz and Bird, 1977), is reasonable at the latitude of this study.

The subducting slab begins its descent at a low angle,

Because the trackline trends east-west and near the equator, the change to the new reference system adds only a small, constant number of milligals to the anomaly. The change is ignored here.

but it bends downward sharply at about 200 km behind the trench (Isacks and Baranzangi, 1977). Deep earthquakes show that it extends to a depth of at least 680 km (Katsumata and Sykes, 1969).

To the west of the volcanic arc lies the Mariana Trough, an active extensional, back-arc basin (Karig, 1971b). It is a region of high heat flow (Anderson, 1975) and anomalously thin lithosphere (Seekins and Teng, 1977). The trough began opening in the Late Miocene (Hussong and Uyeda et al., 1978). The extension occurred as spreading localized about the axial high which runs through the middle of the trough, roughly parallel to the arc (Karig, 1971a). Although the spreading may be similar to that at mid-ocean ridges, it produces no correlatable magnetic anomalies (Karig et al., 1978). Consequently, the total spreading rate is not well known; although, estimates vary from 40 mm/yr (Hussong, Uyeda, et al., 1978) to 80 mm/yr (Karig et al., 1978) on the basis of topography and sediment ages.

DATA

All the data used in this study were collected in February 1976 by the R/V Kana Keoki as a part of the International Phase of Ocean Drilling (IPOD) Mariana site survey. The line A-A, shown in Figure 1, was selected because it is perpendicular to the arc and coincident with the seismic refraction shotline analyzed by LaTraille (1978).

The bathymetry was obtained using conventional echo sounding techniques, with a 3.5 kHz acoustical source, and corrected using Mathhews' (1939) tables. Sediment thicknesses were determined from reflection records obtained with airgun and sparker sources.

The seismic refraction data consist of 29 single-ship, non-reversed profiles. Twenty sonobouy stations were located along a 500 km line west of the trench, and nine were located on a 235 km line east of the trench. Maximum shot-to-receiver distance on each profile was approximately 40 km.

The gravity data were digitized along the seismic refraction line at an interval of 6 km. The data were obtained with a LaCoste-Romberg stable platform gravimeter whose accuracy is ± 1 mgal assuming no navigational errors (LaCoste, 1967). Satellite Doppler positions were used throughout. The methods of Rose and Norris (1971) and Rose (1974) were used to obtain adjusted dead reckoning tracks. The mean crossing error of tracklines in this survey is approximately ± 4 to 5 mgal.

The gravity observations were reduced to free-air anomalies with reference to the International Reference Ellipsoid (Garland, 1965, Heiskanen and Moritz, 1967) with a flattening of 1/297.0. All gravity values were referenced to the harbor bases tied to the International Gravity Base Network of Woollard and Rose (1963). Anomalies based on this older reference ellipsoid may be updated to the new Geodetic Reference System (Woollard, 1979).

THE MODEL

Due to the large number of elements which must be treated in a model of this magnitude, some simplifications were made to facilitate computation. The model was broken into three parts: the crustal layers, the down-going slab, and the low density, back-arc mantle. All of these elements were treated as density anomalies contrasted to a mantle of density 3.35 g/cc. The use of density anomalies not only makes it easier to modify the model, but also allows the model to be independent of any assumed dimensions of the lithosphere and low velocity zone and of the density gradient within the mantle. Thus, the increase of density with depth and the asthenospheric low velocity zone were not modeled, but are implicitly assumed in the density anomalies.

The Crustal Layers

The seismic refraction results of LaTraille (1978) were used to constrain a density model of the crust. Density values were derived by grouping compressional wave velocities, averaging, and converting to density using the velocity-density systematics of Ludwig et al., (1970). The seismic results were jumbled, particularly behind the arc, suggesting broken, non-continuous layers. However, for ease in the computation of the gravity model the crustal layers were smoothed as much as possible without alteration of broad geological relationships.

Though the upper crustal layers are seismically well determined, the Moho is not; Seaward of the trench this presented little problem as the depth to the Moho was found to be consistent. Behind the arc, however, the depth to the Moho was determined only beneath the middle of the Mariana Trough; yet it is likely to vary greatly on either side of this basin due to the roots of the frontal and remnant volcanic arcs.

Other investigators have concluded that a root exists beneath the Mariana arc (Murauchi et al., 1968). Since no Moho velocities were detected beneath the crust of the frontal and remnant arcs at the latitude of this study (LaTraille, 1978), the dimensions of any roots beneath these arcs are uncertain. To be objective, this study first assumed no crustal roots behind the trench. In order to fit the observed gravity anomaly, it was later necessary to assume roots beneath both the Mariana arc and West Mariana Ridge. The result, shown in Figure 2 was similar to previous work (Murauchi et al., 1968), however, it was necessary to add an additional protrusion at the apex of the broad root beneath the frontal arc.

Starting at the eastern end of the transect, the oceanic crust was modeled with a slight compensating Moho depression beneath the seamount and a slight thinning just seaward of the trench prior to its plunging beneath the arc. The subducted crust was assumed to follow the Benioff zone as determined from earthquake hypocenters (Isacks and Barazangi, 1977) and to maintain a constant thickness equal to its pre-subduction thickness.

The layers found east of the trench were modeled separately down the subducting slab to a depth of 30km. From 30-80 km an average density of 2.8 g/cc was assumed. This value was derived from a crustal average of 2.7 g/cc (Hussong, 1972) corrected for thermal expansion and adiabatic compression. The coefficients of expansion and compression used in this approximation correspond to a peridotite composition. The values used were $dV/VdT = 3.6 \times 10^{-5} \text{ } ^\circ\text{C}^{-1}$ (Skinner, 1966), and $dV/VdP = 7.0 \times 10^{-4} \text{ Kbar}^{-1}$ (Birch, 1966).

The Downgoing Slab

To estimate the gravity anomaly due to the dense slab a thermal model for the slab was constructed from a published model (Turcotte and Schubert, 1973) as shown

in Figure 3. This model was selected because it stays relatively cool with depth, consistent with a steeply dipping, fast subducting slab (Miner and Toksoz, 1970) such as is found at the Mariana arc. This model also includes the effect of the olivine-spinel phase change.

From the thermal model a density anomaly model was constructed using the previously mentioned thermal expansion coefficient. Although this coefficient should be reduced with depth (Birch, 1952), its value is not accurately known, so it was considered constant in this study. Compression was not considered in the derivation of the slab model since the pressure is assumed to be hydrostatic.

Figure 3b shows the density anomaly model calculated using the above model. Other investigators have modeled downgoing slabs without resorting to such complicated density models. Often, the slab is modeled with a constant density contrast throughout. Usually, the contrast is about +0.04 to +0.05 g/cc (Hatherton, 1970, Grow, 1973, Getts and Rose 1978). A spatial average of the density anomalies in Figure 3b is almost exactly +0.05 g/cc. A simpler model, Figure 3c, assumes this constant density contrast. As suspected, the gravity anomalies calculated from the density models of Figures 3b and 3c are identical to within the crossing error of the tracks in this study. Consequently the simpler constant density model was used in the construction of the calculated gravity model.

The top of the slab was delineated using earthquake hypocenter results (Katsumata and Sykes, 1969, Isacks and Barazangi, 1977), and a constant slab thickness of 80 km was assumed. This thickness was chosen because it is the value most used in thermal models, including the one used in this study. The exact thickness is uncertain, but is likely to be between 75-100 km (Sclater and Francheteau, 1970). Since there have been no earthquakes detected

below 680 km beneath the arc (Katsumata and Sykes, 1969), the slab was assumed to end at that depth. Should there be any slab below 680 km its great depth would cause its gravity effect to be small at the surface.

In a complex set of dehydration reactions, most of the subducted oceanic crust turns into eclogite at a depth of about 60-80 km (Anderson et al., 1976, Delany and Helgeson, 1978). The eclogite has a density, in situ, of 3.56 g/cc (Grow and Bowin, 1975). In this study the oceanic crust is assumed to change to eclogite at 80 km as shown in Figure 3. For simplicity, the crust below 150 km is assumed to have the same density contrast as the rest of the slab. If the eclogite were continued all the way down the slab, it would add no more than 15 mgal to the gravity anomaly of the slab.

The Low Density Mantle:

Figure 2 shows the consequences of assuming that the mantle beneath the Mariana Trough is of the same density (3.35 g/cc) as the mantle beneath the Pacific plate. The calculated anomaly is too high by 170 mgal. A reasonable cause of this discrepancy may be the occurrence of low density mantle beneath the center of the Mariana Trough.

Figure 2 also shows that the maximum anomaly due to the low density mantle must be approximately centered on the axial high. That this is also the center of spreading in the trough is not a coincidence, for this should also be where melt is shallowest beneath the basin. There has been slight disagreement as to the exact placement of the locus of spreading. Karig (1971a) puts it at the axial high, while Hussong, Uyeda, et al., (1978) place it at a graben about 30 km to the east.

However, the lack of information on the back-arc Moho makes the position of the anomaly too dependent on the assumed Moho to be diagnostic as to the position of the center of the anomaly. Consequently, in the model

the low density mantle anomaly is arbitrarily centered on the axial high.

There are few constraints on the shape and density contrast of the anomalous mantle. The back-arc lithosphere is known to be thin (Seekins and Teng, 1978) and spreading occurs in the center of the trough (Karig et al., 1978).

In an effort to make the simplest reasonable approximation, the anomalous body is assumed to have the same density contrast throughout. The lithosphere is modeled thickening away from the center of the basin, much like the lithosphere at a mid-ocean ridge. Since the mechanism of spreading in the Mariana Trough is unknown, this may not be a good analogy (Karig et al., 1978). The base of the lithosphere is assumed to approximate the 1100°C isotherm of Andrews and Sleep's (1974) thermal model. This temperature should be the wet solidus of the lithospheric material (Yoshii et al., 1976).

Two other configurations of the low density mantle were tried as well. In one of these models, the low density mantle was extended to the corner between the sub-arc root and the descending slab. This configuration roughly corresponds to the tectonic model of Kanamori (1977). The other model assumed that the eastern side of the low density mantle is vertical and located at the volcanic axis. This configuration might be the result of an island arc, lithospheric block being carried seaward by the spreading in the Mariana trough as suggested by Karig's (1971a) model. Either of these models can be made to work as well as the one shown in Figure 4. The former necessitates a slight shallowing of the Moho beneath the arc, and the latter, a slight deepening of the Moho. Due to the lack of information on the placement of the sub-arc Moho, gravity alone cannot be used to determine which of these models is best.

A variety of depths to the bottom of the low density mantle have been used in the literature, so a number of

different depths were also tried in this study. The density contrast was adjusted to fit the observed anomaly once the depth to the bottom of the low density mantle was chosen. Table 1 lists the density contrasts which correspond to different assumed depths. Figure 6 shows the anomalies calculated using these values. The 100 km anomaly decreases rapidly away from the trough's axial high. In order to use this depth, the roots beneath the frontal and remnant arcs must be significantly deepened. Conversely, the 400-500 km depths provide such a broad anomaly that these roots must be made significantly shallower. Thus, the models using these depths to the bottom of the low density mantle were rejected. If the depth of the back-arc Moho were accurately known, perhaps the depth of the lower bound of the anomalous mantle could be more accurately determined. The model presented in the figures assumes an arbitrary depth of 200 km to the bottom of the anomalous mantle with a density contrast of -0.033 g/cc.

In Figure 2, the calculated anomaly assuming a mantle of 3.35 g/cc beneath the trough falls off rapidly with distance west of the axial high. It is assumed that this effect is due both to the root beneath the West Mariana Ridge and due to the western edge of the low density mantle. Thus, the low density mantle is arbitrarily assumed to end beneath the West Mariana Ridge, as shown in Figure 4.

To arrive at a calculated gravity anomaly, the contribution from the crust and downgoing slab are added. The density of the back-arc mantle is adjusted to make the calculated anomaly match the observed anomaly over the trough. In a similar manner, the shape of the sub-arc root is adjusted to fit the anomaly over the arc and fore-arc regions. The calculated anomaly is shown in Figure 2. In Figure 5 the major, calculated positive and negative anomalies are shown. The downgoing slab contributes $+140$ mgal in a broad positive anomaly. This anomaly increases the gravi-

tational attraction over the arc and trough. The -170 mgal negative due to the low density mantle compensates for the positive slab anomaly and for the positive anomaly due to the shallow mantle beneath the trough.

In order to compare the observed and calculated gravity anomalies, the two must be registered at some point along the traverse. Often, this is accomplished by matching the anomalies at the seaward end of the line. However, in this study, that point is over one of the Magellan seamounts. This problem proved to be small, for the anomaly calculated from the crustal model, east of the trench, fit the observed anomaly with little adjustment.

TABLE 1: Depths and densities of the low density mantle.

If one of the following depths is chosen as the bottom of the low density mantle, then the corresponding density anomaly is required for the model to fit the observed gravity.

depth (km)	Density Anomaly
100	-0.057
200	-0.033
300	-0.028
400	-0.024
500	-0.022

DISCUSSION

The observed free air anomaly (FAA) is shown in Figure 2. As expected, it follows the bathymetry closely. A broad bulge is to be seen in the FAA between the trench and the seamount. It is probably due largely to an edge effect from the thick crust beneath the seamount. However, it may also be partially due to an outer gravity high caused by lithospheric flexure (Watts and Talwani, 1974).

Behind the trench, the FAA rises slowly from the trench-slope break to the axial high of the trough. Landward of the axial high, the FAA decreases. At the location of the volcanic axis, approximately 220 km behind the trench, the FAA rises about 50 mgal. West of that point over the trough, the FAA is rough and somewhat elevated above the level set by the fore-arc region.

Figure 2 also shows that the calculated anomaly matches the FAA well east of the trench. Except for one large (40-50 mgal) bump about 100 km behind the trench, the model anomaly fits the observed anomaly well over the fore-arc region. The large amplitude and short wavelength of the bump suggest a shallow, dense causative body which is unaccounted for by the crustal model. In a plan view this bump is circular and thus cannot be treated by two dimensional modeling. Since it has no apparent bearing on the regional structure, this anomaly will be discussed no further in this study. Over the Mariana Trough the observed and calculated anomalies do not always match, probably due to the rough bathymetry of the trough which violates the two dimensional assumption of the gravity modeling.

An interesting structure is inferred in the crust behind the trench. Because the gravity low at the trench is offset slightly landward from the bathymetric low, a

low density wedge is inferred in the crust behind the west wall of the trench. The assumed density is 2.4 g/cc similar to that of accreted sediments found in other arcs (Grow, 1973). The dimensions of this wedge are arbitrary and it is somewhat smaller than other such wedges. Unfortunately, there is no other geophysical or geologic evidence to determine the nature of this low density wedge. It might be a sedimentary accretionary prism, a zone of highly sheared crystalline rock, or some other geologic feature.

The shape of the sub-arc root is also of interest. It is notably asymmetric about the volcanic axis of the arc. The slope of the west side is approximately 14 degrees while the slope of the east side is only 4 degrees. Figure 2 shows an odd protrusion at the apex of the root. It is 4 km deep and 36 km in length. Although the shape of this feature is poorly defined by the modeling technique, its general dimensions are similar to the magma chambers found at moderate depth beneath the Katmai range of the Aleutian arc (Kubota and Berg, 1967) and beneath the volcanoes of Kamchatka (Utnasin et al., 1976). The transect of this study passes between two volcanic islands, Alagan and Pagan, which are nearly 50 km apart. One might not expect to find a magma chamber beneath the saddle between two volcanoes; however, the seismic results from the Katmai Range suggest that the deeper magma bodies may be elongated parallel to the arc (Kubota and Berg, 1967). Perhaps this sub-root structure is an expression of a moderately deep magma chamber beneath the Mariana arc.

Few investigators have attempted to model the low density mantle beneath active, extensional back-arc basins (Soloman and Biehler, 1969, Karig, 1971b, Segawa and Tomoda, 1976). The diversity amongst these models reflects a lack of constraining data. Solomon and Biehler's (1969) model of the New Hebrides arc (which will be referred to as model 1) extends the low density mantle, with a density

contrast of -0.03 g/cc, from the Moho to a depth of 100 km. Laterally, the anomalous mantle stretches indefinitely landward from a nearly vertical line beneath the trench. This model ignores the gravity anomalies associated with the downgoing slab and the subducted oceanic crust. The Karig model (1971b) (model 2), designed with the Mariana Trough in mind, used a body of anomalous mantle with vertical sides located at the edges of the trough. The low density mantle, with a density anomaly of -0.02 g/cc, extends from the Moho to a depth of 300-400 km. This model does not attempt to match the observed gravity anomaly exactly, so it also ignores the slab and subducted crust anomalies. The Japan Sea models of Segawa and Tomoda (1976) (generalized as model 3) do include the gravity anomaly associated with the downgoing slab, however, they also fail to account for the effect of the subducted crust. These models assume a back-arc lithosphere with a constant thickness of 30 km. The anomalous mantle, with a density contrast of -0.015 to -0.02 g/cc, is beneath the lithosphere extending to a depth of 150 km. These models have no landward limit to the low density mantle, which is also extended seaward into the corner between the sub-arc root and the descending slab.

The model used in this study was designed with the good and bad points of models 1-3 in mind. Although this model is not unique, every effort has been made to make it reasonable in the light of current geophysical knowledge. Figure 2 shows that the anomaly due to the low density mantle should be maximum over the center of the trough. Even though Karig (1971b) first suspected this type of anomaly, no model has yet been constructed in this manner. Models 1-3 all have a flat top to the anomalous mantle which does not concentrate the anomaly in the center of the basin. Also, these models have incorrectly represented the mantle and crust laterally. Models 1 and 3 have made the unlikely assumption that the anomalous mantle extends

indefinitely westward. Also, model 3 extends the marginal sea crust indefinitely westward. Because of these features, the anomaly due to the low density mantle in these models does not fall off behind the basin. Beneath the arc, models 1 and 2 show no subducting slab. Consequently, the amplitude of the anomaly over the basin is not high enough. None of these models account for the subducted oceanic crust, hence, the anomaly does not fall off towards the trench. Probably, this incorrect modeling of the descending oceanic crust has caused the authors of models 1 and 3 to extend the low density mantle as far towards the trench as they have. The model used in this study contains the subducting crust and slab, and it has the thinnest back-arc lithosphere beneath the locus of spreading, also it bounds the low density mantle westward beneath the West Mariana Ridge.

CONCLUSIONS:

The results of this study tend to substantiate the work of other investigators who have suggested the existence of large amplitude, large wavelength gravity anomalies associated with the downgoing slab and low density mantle beneath the Mariana trough. Also, the character of the gravity anomaly over the Pacific plate supports the existence of an outer gravity high between the trench and the Magellan seamounts. The exact cause of the outer gravity high is still uncertain, but it is modeled here as a slight thinning of the crust. The gravity data also require roots beneath the remnant arc and frontal volcanic arc, even though these were not detected by seismic refraction in the area.

Several interesting anomalies were noted in the crust west of the trench. A low density wedge is postulated behind the landward wall of the trench. The root beneath the frontal arc is asymmetric with respect to the volcanic axis of the arc. The sides of the sub-arc root have different slopes and the center of the root is offset toward the trench from the axis of the volcanoes. Also, it is necessary to add a sub-root at the apex of the sub-arc root. Its dimensions suggest that it might be a magma chamber of moderate depth.

The anomaly due to the low density back-arc mantle was found to fall off away from the axial high of the Mariana Trough. Consequently, the back-arc lithosphere was modeled thickening away from the axial high. As well, the low density mantle was bounded on the west beneath the west Mariana Ridge. It was impossible to determine the exact depth to which the low density mantle stretches however, it was judged to be between 100-400 km.

APPENDIX

LOW DENSITY, BACK ARC MANTLE ANOMALIES CALCULATED FROM MODELS

A number of investigators have constructed thermal models which claim to reproduce the elevated isotherms beneath an active, extensional back-arc basin. To my knowledge, no one has calculated the gravity anomalies associated with the anomalous back-arc basin. Just such a test should be able to distinguish which thermal models are most reasonable in terms of their gravity effect.

Several thermal models were tested by adapting them for use in a two dimensional gravity model of the Mariana Trough. One model assumes that the back-arc isotherms are displaced towards the surface by a cell of convective counter-flow in the upper mantle due to the drag of the down-going slab (Andrews and Sleep, 1974). Another model assumes the cause of the temperature anomaly to be the effect of magma rising from the Benioff zone (Sydora et al., 1978). Yet another model is an estimate of the elevation of the back-arc isotherms and it assumes no specific mechanism for raising the isotherms (Schubert et al., 1975). All of these models assume a slab dipping at 45 degrees, but each assumes a different subduction velocity. The slab of Andrews and Sleep's (1974) model has a velocity of 100 mm/yr; Schubert et al.'s (1975) model, 80 mm/yr; and Sydora et al.'s (1978) model, 10 mm/yr.

Figures A1, A2 and A3 show the density anomalies derived from these thermal models. The density anomalies were calculated using the temperature anomalies caused by the elevated isotherms with a thermal expansion coefficient of $3.6 \times 10^{-5} \text{ }^{\circ}\text{C}^{-1}$ (Skinner, 1966). The gravity anomaly associated with each of these density anomalies was substituted for the block of low density mantle used in previous calculations. The anomaly was centered on the axial high of the trough.

These density models are different from the previously used low density mantle model in that these concentrate the largest density anomaly beneath the center of the basin. The lesser density anomalies form shells around the larger density anomaly. In the model used previously, a uniform density was assumed throughout the low density mantle body.

Figure A4 compares the gravity anomalies calculated for the Mariana Trough, using no low density mantle and using these three density models, to the observed gravity. When no low density mantle is used in the model, the gravity anomaly is too high over the trough by 170 mgal. Using the model of Schubert et al. (1975), the calculated gravity is too high by 100 mgal; and with the model of Andrews and Sleep (1974), it is too high by 50 mgal. Thus both of these models have too little elevation of the isotherms beneath the Mariana Trough. With the Andrews and Sleep (1974) model, this problem can be easily fixed by extending the -0.01 g/cc body of the density model to a depth of 200 km. On the other hand, the gravity anomaly due to the Sydora et al. (1978) model is much too large and broad. With this model, the calculated gravity over the trough is too low by 40 mgal. Also, the anomaly reduces the calculated gravity too much over the West Mariana Ridge and over the arc-trench gap. If the density anomalies are not substantially reduced in size, then major modifications of the crustal layers would be needed in these areas to make this model work.

An obvious question to ask is whether the gravity can be used to distinguish which mechanism causes the elevation of the isotherm beneath the Mariana Trough. This question assumes that there is a fundamental difference between the anomalies caused by the counter-flow model and the rising magma model. It is not certain that there is any such fundamental difference. In the published models, the counter-flow anomaly (Andrews and Sleep, 1974)

is much smaller than the massive anomaly due to the rising magma model (Sydora et al., 1978) It is quite possible that the difference between these two models is merely due to the different initial conditions and dimensions of the models. The gravity results are certainly inconclusive in determining the superiority of either model, for the Andrews and Sleep (1974) model gives an anomaly which is too small, and the Sydora et al. (1978) model gives an anomaly which is too large.

Fig. 1. Map of the study area. The line A-A is the transect analyzed in this report. The contours are at 3000m intervals. The hatched areas are deeper than 6000m. The map is modified from Karig (1971a).

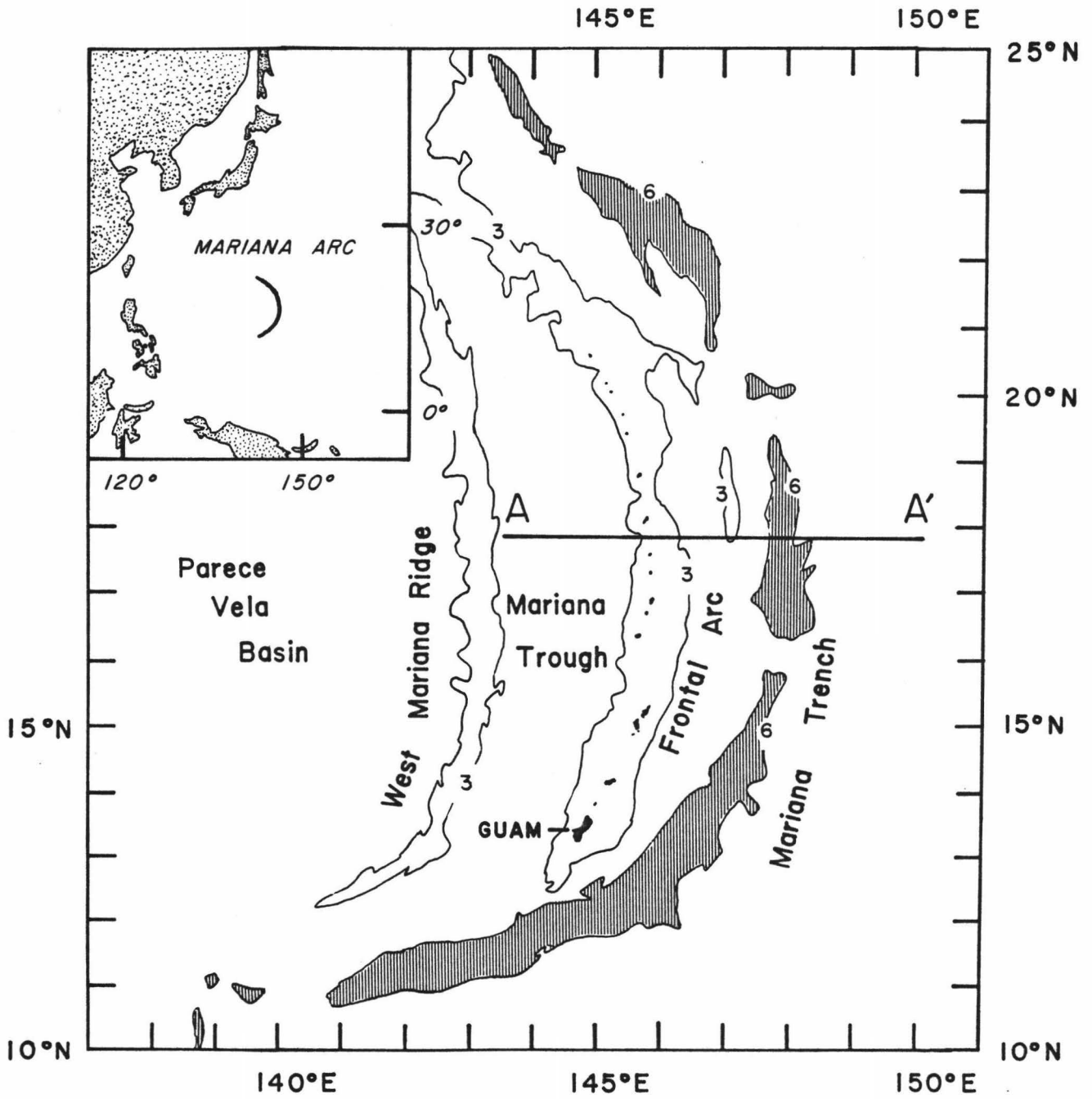


Fig. 2. The observed and calculated gravity anomalies and the crustal model.

top: The solid curve is the observed free air anomaly. The dots represent the anomaly calculated from the crustal slab, and low density mantle models. The x's represent the same model without the low density mantle beneath the Mariana Trough.

bottom: The solid lines are crustal layers determined from seismic refraction results (LaTraille, 1978) and the dashed lines represent inferred surfaces. The densities are in grams per cubic centimeter. The apparent thinning of the subducted crust is an artifact of the 12:1 vertical exaggeration.

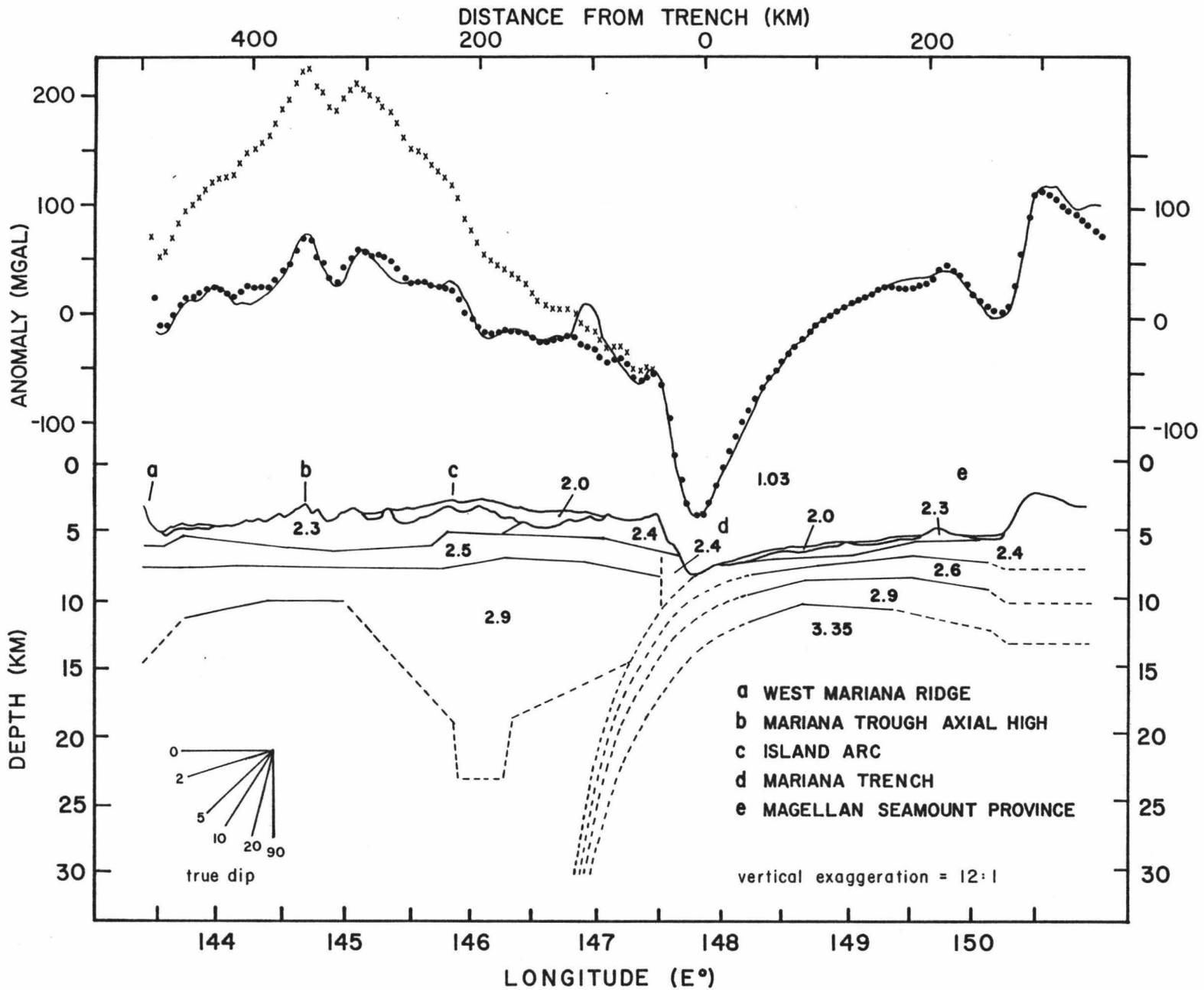


Fig. 6. The gravity anomalies which correspond to the low density mantle model of Table 1. The numbers 100-500 correspond to the assumed depth of the bottom of the anomalous mantle used in the calculation of that curve.

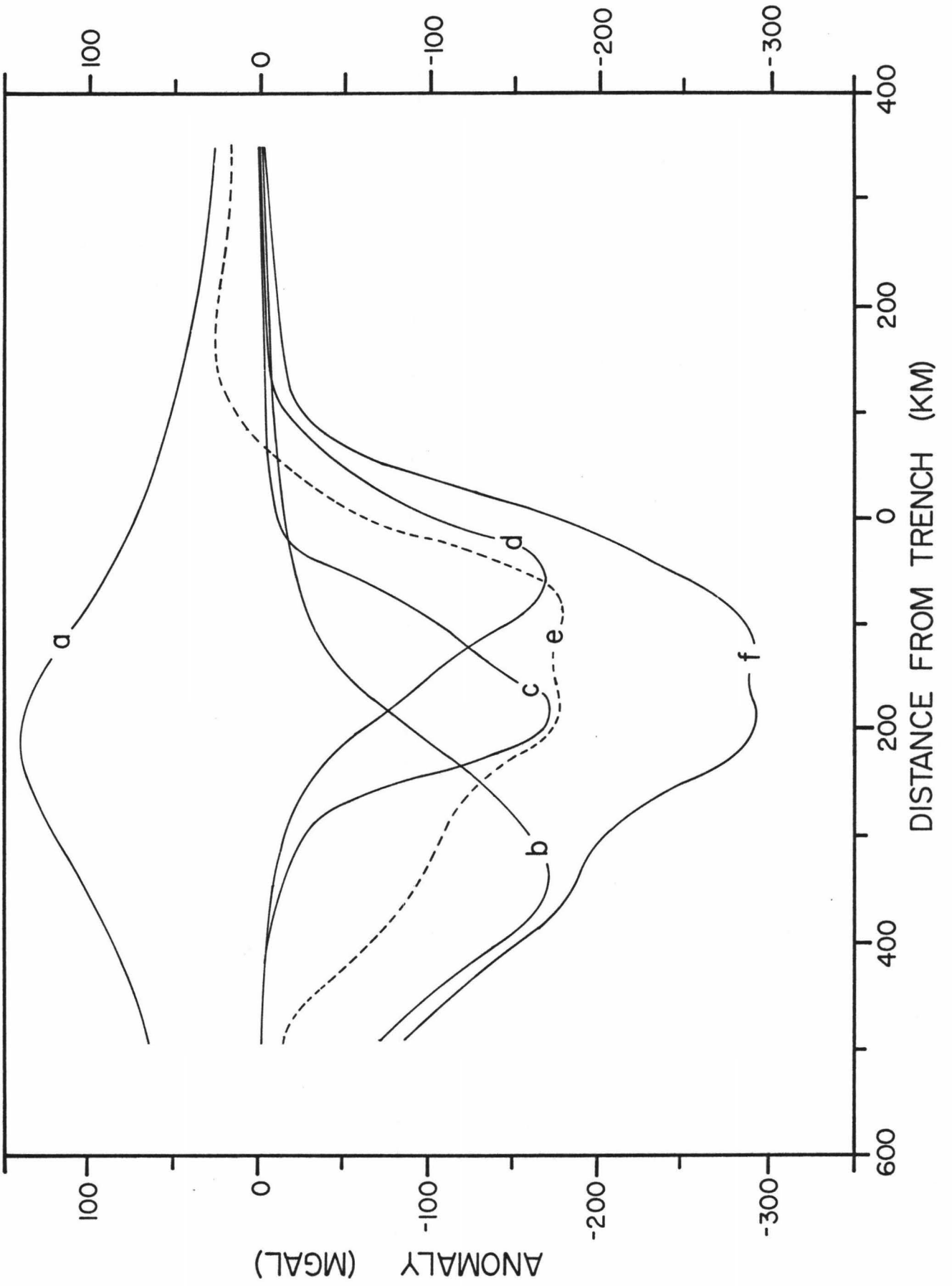


Fig. 5. Gravity anomalies from major bodies in the model. Curve a is the anomaly due to the downgoing slab. Curves b,c, and d are from the low density mantle, sub-arc root, and the subducted oceanic crust. The sum of b,c, and d are plotted in curve f. Curve e is the sum of curves a and f.

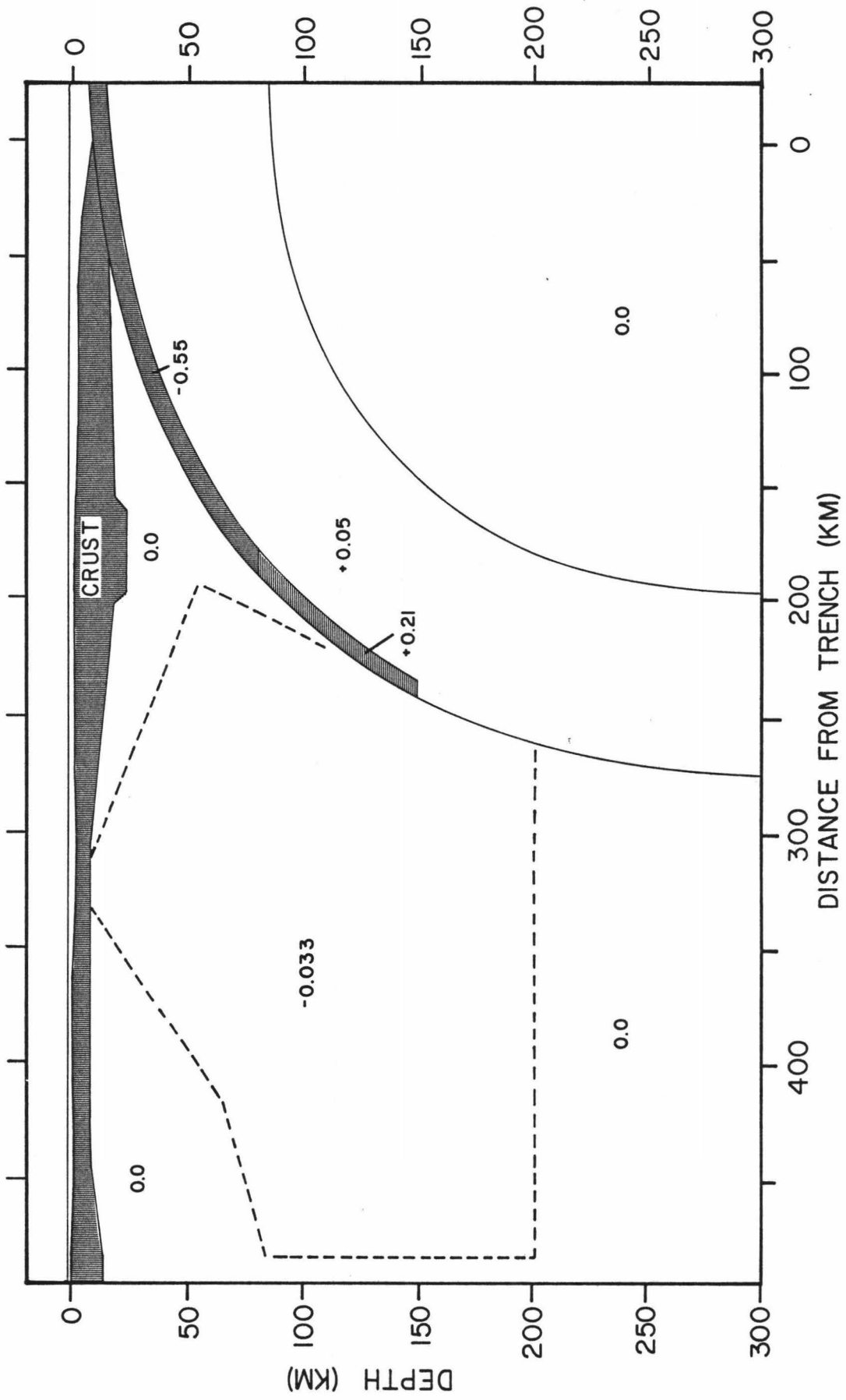


Fig. 4. The low density mantle model. The anomalous mantle is assumed to be the same density contrast throughout. The upper surface roughly follows the 1100°C isotherm of the back-arc thermal model of Andrews and Sleep (1974). The depth to the bottom of the body is 200 km and the density anomaly is -0.033 grams per cubic centimeter; although, other depths and density contrasts, as listed in table 1, were tried as well.

Fig. 3. The downgoing slab model. The slab follows the earthquake hypocenters determined by Isacks and Barazangi (1977) and Katsumata and Sykes (1969).

a: The slab isotherms are derived from the the model of Turcotte and Schubert (1973). The units are in thousands of degrees centigrade.

b: The density model was derived from the thermal model using thermal contraction as described in the text. The density anomalies are in units of grams per cubic centimeter. The hatched areas are density anomalies due to the subducted crust before and after it changes to eclogite.

c: This density anomaly model gives results virtually identical to that of the model in b.

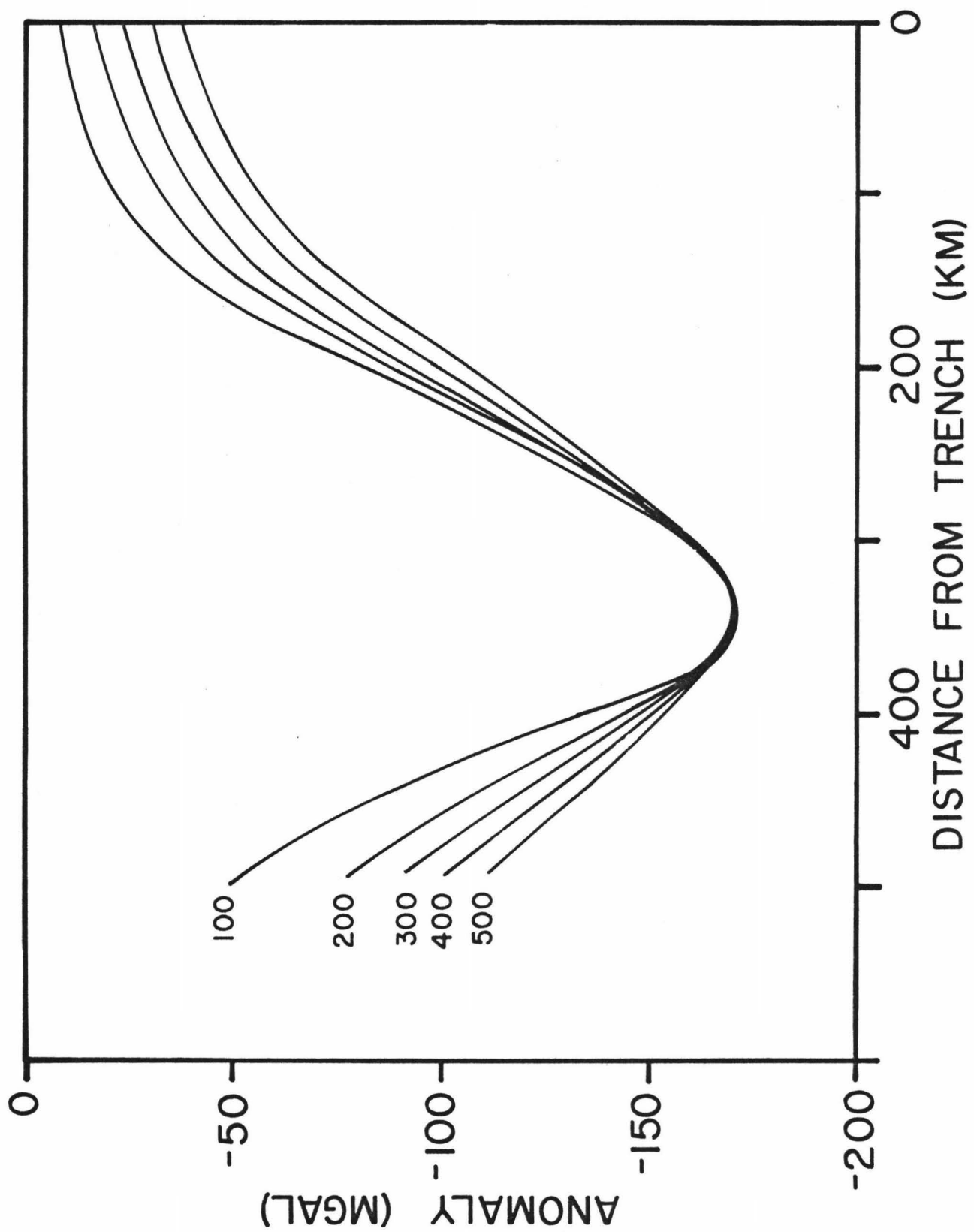


Fig. A1: The density anomaly model derived from the thermal model of Andrews and Sleep (1974). The shaded areas represent the crust and downgoing slab. The solid lines are isotherms, and are labelled in thousands of degrees centigrade. The dashed are the borders of the density anomalies, which are labelled in grams per cubic centimeter.

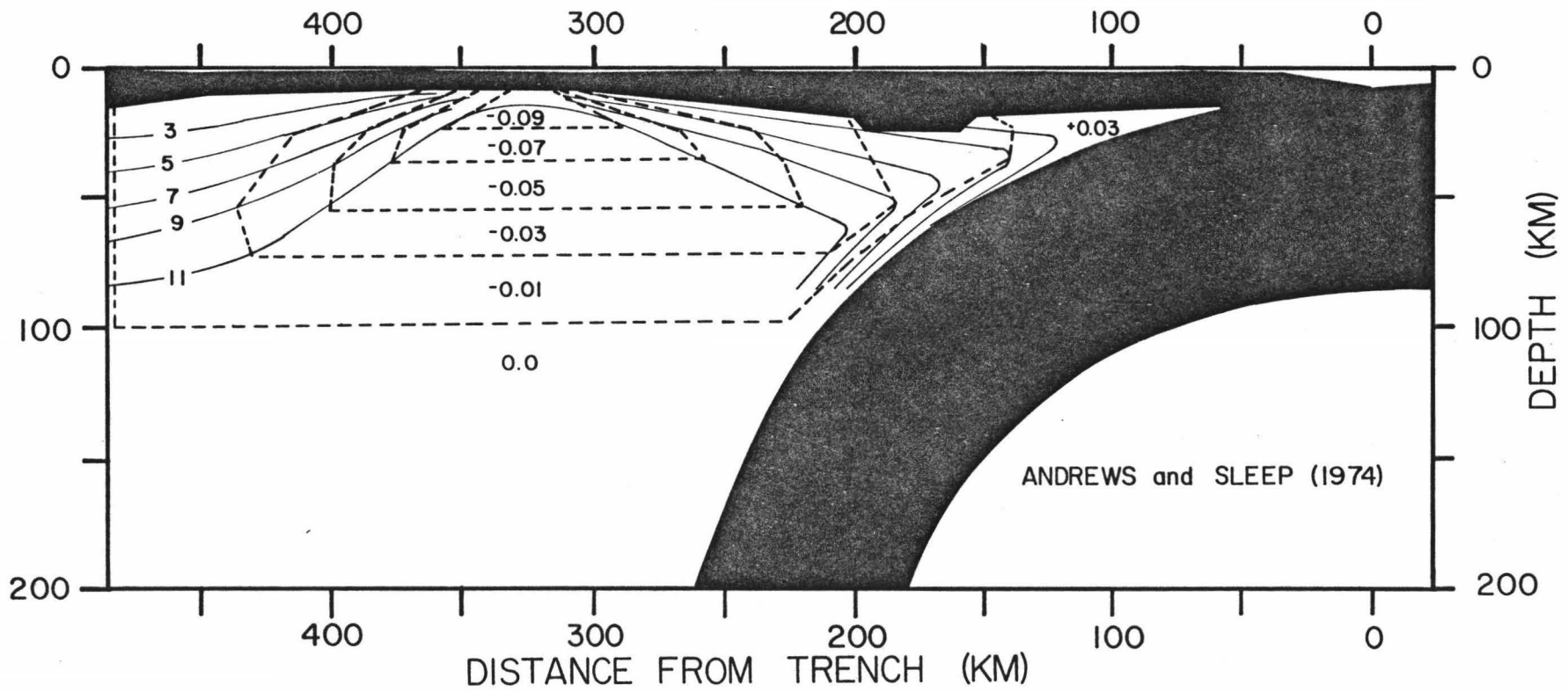


Fig. A2: The density anomaly model derived from the thermal model of Schubert et al. (1975). The above figure is labelled as in figure A1.

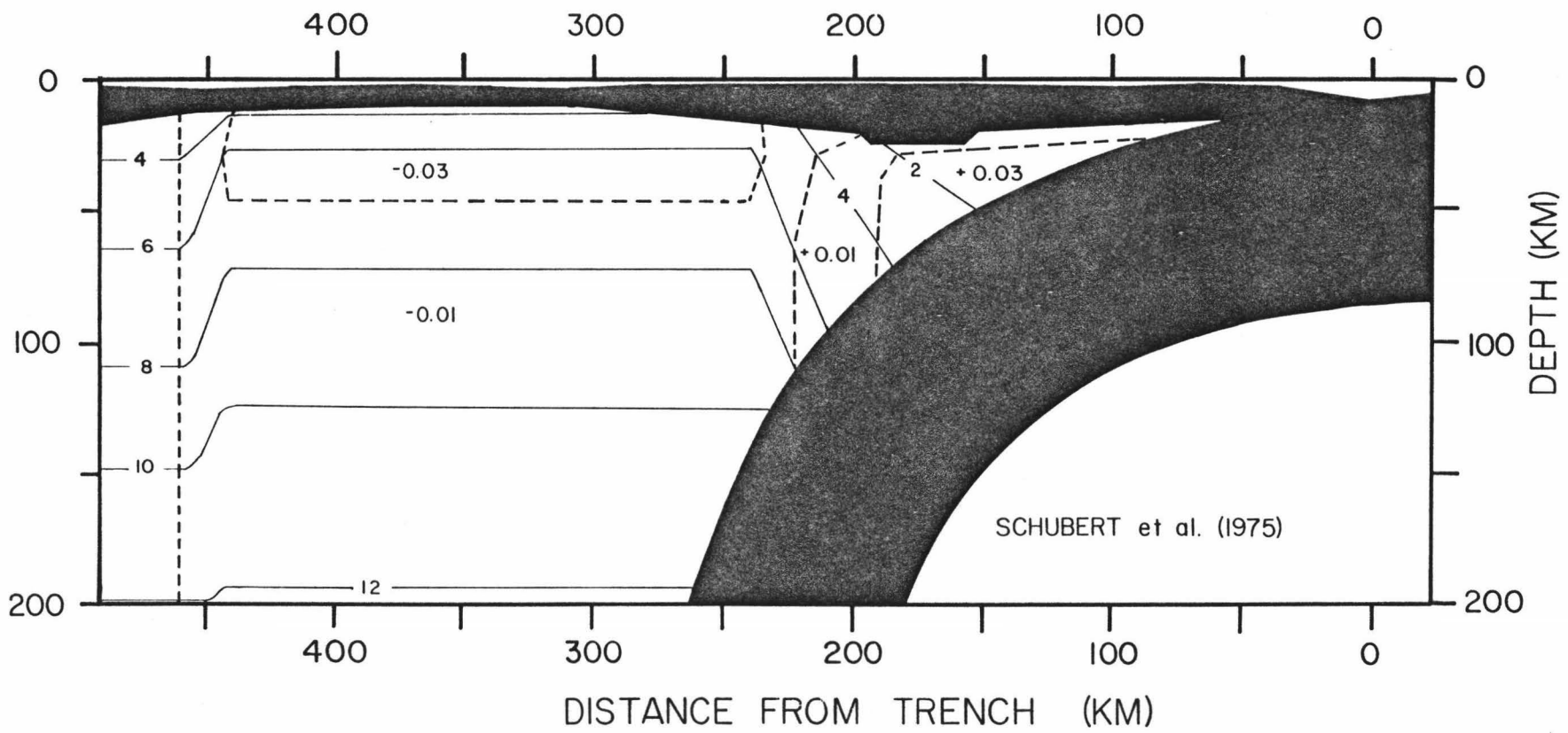


Fig. A3: The density anomaly model derived from the thermal model of Sydor~~a~~ et al. (1978).
The above figure is labelled as in figure A1.

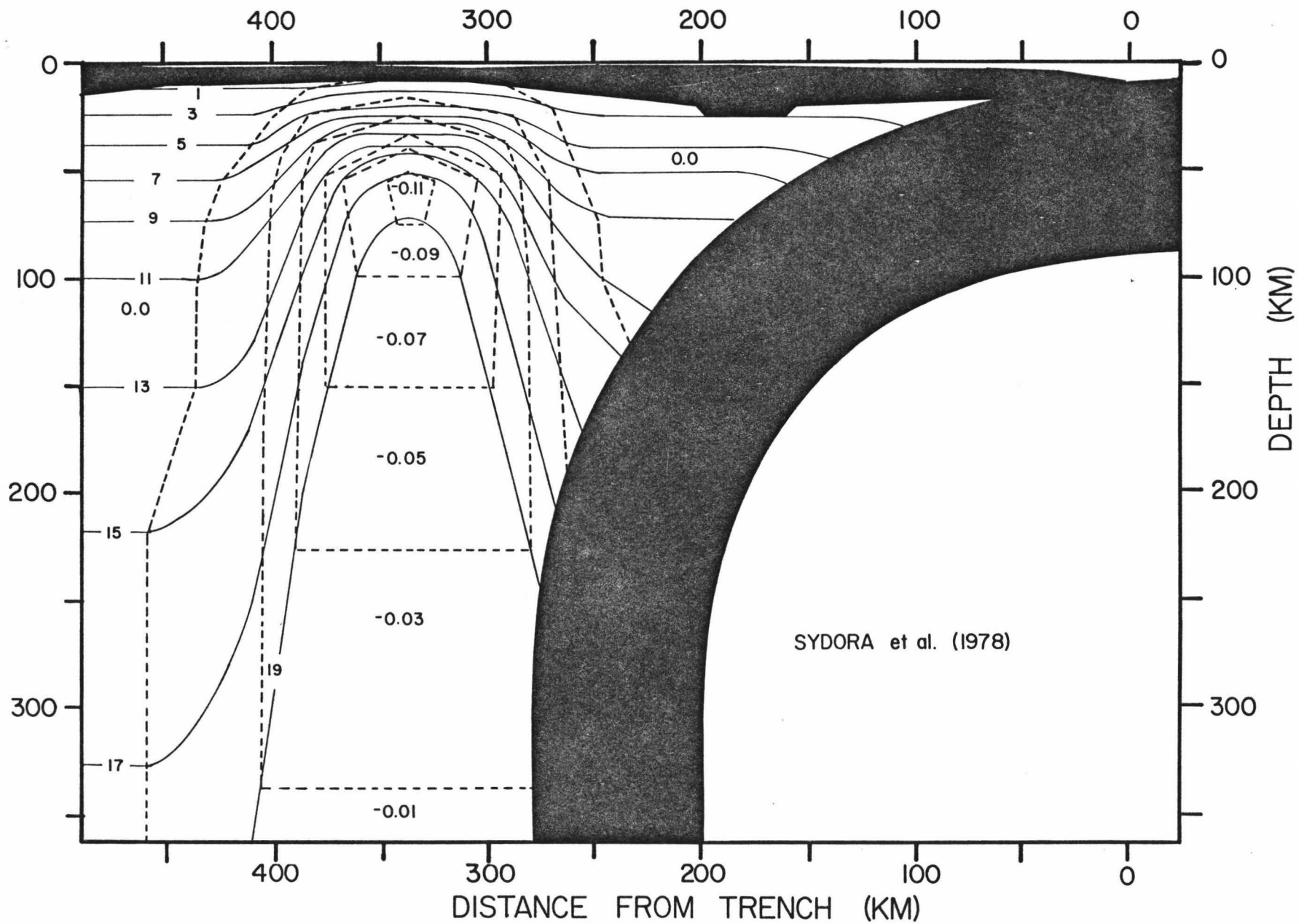
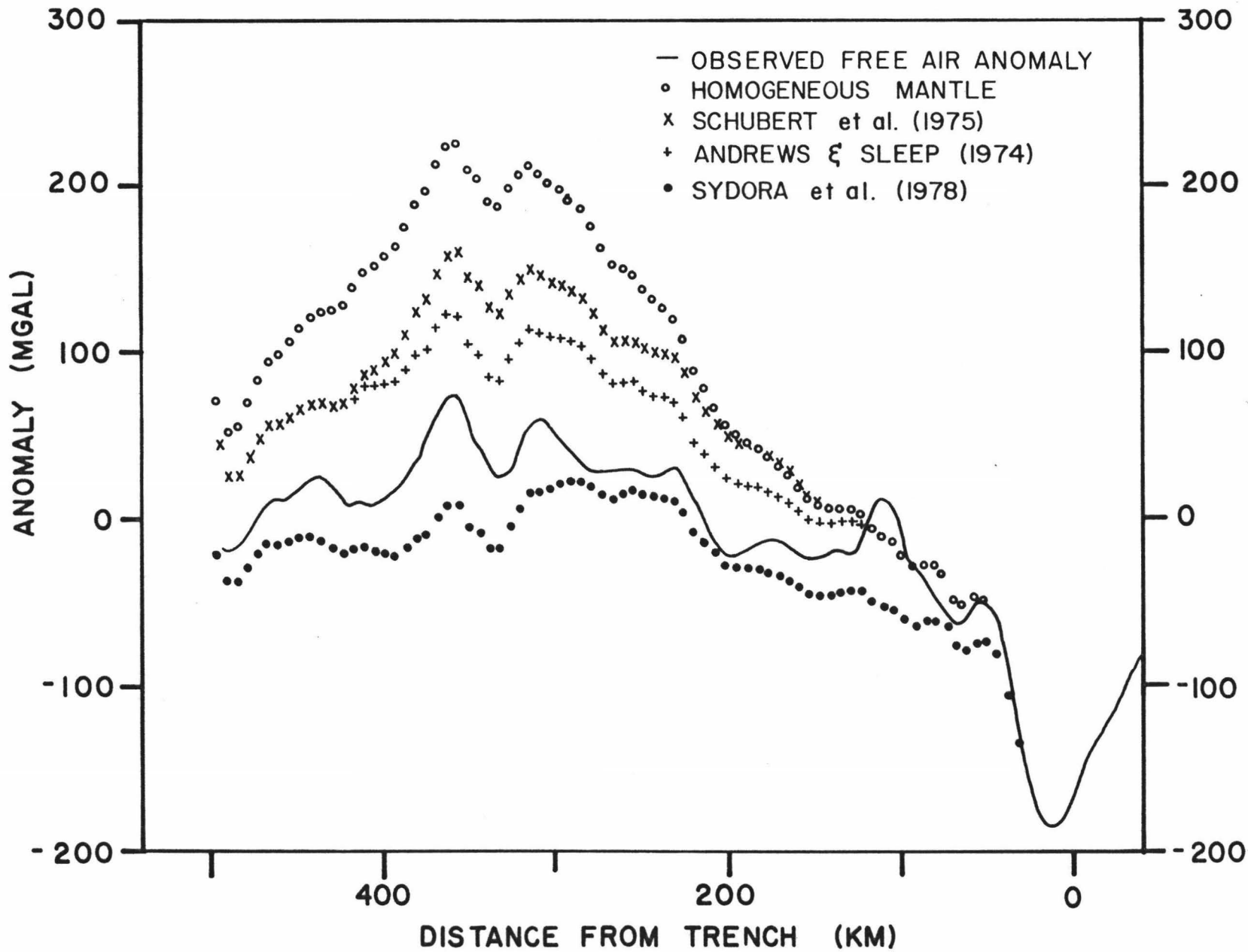


Fig. A4: A comparison of the gravity calculated over the Mariana trough using several different thermal models. The solid line represents the observed free air anomaly and the open circles represent the gravity anomaly calculated using no low density mantle beneath the trough. The x's show the calculated gravity using the model of Schubert et al. (1975) (figure A2) and the +'s are the calculated gravity using Andrews and Sleep (1974) (figure A1). The dots represent the gravity anomaly calculated using the model of Sydora et al. (1978) (figure A3).



REFERENCES:

- Anderson, Roger N., Heat flow in the Mariana marginal basin, J. Geophys. Res., 80, 4043-4048, 1975.
- Anderson, R.N., Seiya Uyeda, and Miyashiro Akiho, Geochemical constraints at converging plate boundaries--part I: dehydration in the downgoing slab, Geophys. J. Roy. Astr. Soc., 44, 333-357, 1976.
- Andrews, D. J. and N. H. Sleep, Numerical modeling of tectonic flow behind island arcs, Geophys. J. Roy. Astr. Soc., 38, 237-251, 1974.
- Birch, Francis, Elasticity and constitution of the earth's interior, J. Geophys. Res., 57, 227-286, 1952.
- Birch, Francis, Compressibility: elastic constants, in Handbook of Physical Constants, Geol. Soc. Amer. Mem. 97, edited by S.P. Clarke, pp. 97-173, 1966.
- Delany, Joan M. and Harold C. Helgeson, Calculation of the thermodynamic consequences of dehydration in subducting oceanic crust to 100 kb and $> 800^{\circ}\text{C}$, Amer. J. Sci., 278, 638-676, 1978.
- Garland, G. D., The Earth's Shape and Gravity, Pergamon Press, Oxford, England, pp. 37-38, 1965.
- Getts, T. R. and J. C. Rose, Crustal and upper mantle structure across the Peru-Chile trench, preprint, 1978.
- Griggs, D.T., The sinking lithosphere and the focal mechanism of deep earthquakes, in Nature of the Solid Earth, edited by Eugene C. Robertson, McGraw-Hill, New York, pp. 361-384, 1972.
- Grow, J. A., Crustal and upper mantle structure of the central Aleutian arc, Geol. Soc. Amer. Bull., 84, 2169-2192, 1973.
- Grow, John A. and Carl O. Bowin, Evidence for high density crust and mantle beneath the Chile trench due to the descending lithosphere, J. Geophys. Res., 80, 1449-1458, 1975.
- Hasebe, K., N. Fujii, and S. Uyeda, Thermal processes under island arcs, Tectonophysics, 10, 335-355, 1970.
- Hatherton, T., Gravity and seismicity of asymmetric active regions, Nature, 221, 353, 1969.

- Hatherton, Trevor, Upper mantle inhomogeneity beneath New Zealand: surface manifestations, J. Geophys. Res., 75, 269-284, 1970.
- Heiskanen, W. A. and H. Moritz, Physical Geodesy, W. H. Freeman and Co., San Francisco, pp. 79-80, 1967.
- Hussong, D. M., Detailed structural interpretations of the Pacific oceanic crust using ASPER and ocean-bottom seismometer methods, Ph. D. dissertation, Univ. Hawaii, 165 pp., 1972.
- Hussong, D. M., S. Uyeda, and DSDP scientific staff, Deep Sea Drilling Project: Leg 60, Geotimes, 23, 19-22 1978.
- Isacks, Bryan L. and Muawia Barazangi, Geometry of Benioff zones: lateral segmentation and downwards bending of the subducted lithosphere, in Island Arcs, Deep Sea Trenches, and Back Arc Basins, Ewing vol. 1, edited by M. Talwani and W. C. Pittman III, pp. 99-111, AGU, 1977.
- Isacks, Bryan, Jack Oliver, and Lynn R. Sykes, Seismology and the new global tectonics, J. Geophys. Res., 73, 5855-5899, 1968.
- Kanamori, Hiroo, Seismic and aseismic slip along subduction zones and their tectonic implications, in Island Arcs, Deep Sea Trenches, and Back Arc Basins, Ewing vol. 1, edited by M. Talwani and W. C. Pittman III, pp. 163-174, AGU, 1977.
- Karig, Daniel E., Structural history of the Mariana island arc system, Geol. Soc. Amer. Bull., 82, 323-344, 1971a.
- Karig, D. E., Origin and development of marginal basins in the Western Pacific, J. Geophys. Res., 76, 2542-2561, 1971b.
- Karig, D. E., Roger N. Anderson, and L. D. Bibee, Characteristics of back-arc spreading in the Mariana trough, J. Geophys. Res., 83, 1213-1226, 1978.
- Katsumata, Mamoru and Lynn R. Sykes, Seismicity and tectonics of the western Pacific: Izu-Mariana-Caroline and Ryukyu-Taiwan regions, J. Geophys. Res., 74, 5923-5948, 1969.
- Kubota, S. and E. Berg, Evidence for magma in the Katmai volcanic range, Bull. Volcanol, ser. 2, 31, 175-214, 1967.

- LaCoste, L. J. B., Measurement of gravity at sea and in the air, Rev. Geophys., 5, 477-526, 1967.
- LaTraille, Sharon L., Crustal structure of the Mariana island arc system and old Pacific plate from seismic refraction data, M. S. Thesis, Univ. Hawaii, 136 pp. 1978.
- Ludwig, W. J., J. E. Nafe, and C. L. Drake, Seismic refraction, in The Sea vol. 4, part 1, edited by E. C. Bullard and A. E. Maxwell, Wiley-Interscience, New York, pp. 53-84, 1970.
- Matthews, D. J., Tables of the velocity of sound in pure water and sea water for use in echo-sounding and sound ranging, second edition, Admiralty Hydrographic Dept., H. D. 282, 52 pp., 1939.
- McKenzie, D. P., Temperature and potential temperature beneath islands, Tectonophysics, 10, 357-366, 1970.
- Minear, John W. and M. Nafi Toksoz, Thermal regime of a downgoing slab and new global tectonics, J. Geophys. Res., 75, 1397-1419, 1970.
- Murauchi, S., N. Den, S. Asano, H. Hotta, T. Yoshii, T. Asanuma, K. Hagiwara, K. Ichikawa, T. Sato, W. J. Ludwig, J. I. Ewing, N. T. Edgar, and R. E. Houtz, Crustal structure of the Philippine Sea, J. Geophys. Res., 73, 3143-3171, 1968.
- Oxburgh, E. R. and D.L. Trucotte, Thermal structure of island arcs, Geol. Soc. Amer. Bull., 81, 1665-1688, 1970.
- Rose, J. C., Open ocean navigation accuracy considerations for marine gravity requirements, in Proc. Int. Symp. Applic. Mar. Geod., Marine Technology Society, pp. 113-122, 1974.
- Rose, J. C. and R. A. Norris, 1971 marine gravity results in the north Pacific on R/V Kana Keoki, in Hawaii Inst. Geophys. report HIG-71-19, Univ. Hawaii, pp. 50-72, 1971.
- Schubert, Gerald, David A. Yuen, and Donald L. Turcotte, Role of phase transitions in a dynamic mantle, Geophys. J. Roy. Astr. Soc., 42, pp. 705-735, 1975.
- Sclater, J. G. and J. Francheteau, The implications of terrestrial heat flow observations on current tectonic and geochemical models of the crust and upper mantle of the earth, Geophys. J. Roy. Astr. Soc., 20, 509-542, 1970.

- Seekins, Linda C. and Ta-Liang Teng, Lateral variations in the structure of the Philippine Sea plate, J. Geophys. Res., 82, 317-324, 1977.
- Segawa, Jiro and Yoshibumi Tomoda, Gravity measurements near Japan and study of the upper mantle beneath the oceanic trench--marginal sea transition zones, in the Geophysics of the Pacific Ocean Basin and its Margin, Geophys. Mon. Ser., vol. 19, edited by George H. Sutton, Murli H. Manghnani, and Ralph Moberly, pp. 35-52, AGU, 1976.
- Skinner, Brian J., Thermal expansion, in Handbook of Physical Constants, Geol. Soc. Amer. Mem. 97, edited by S. P. Clarke, pp. 75-96, 1966.
- Solomon, S. and S. Biehler, Crustal structure from gravity anomalies in the southwest Pacific, J. Geophys. Res., 74, 6696-6701, 1969.
- Sydora, L. J., F. W. Jones, and R. St. J. Lambert, The thermal regime of the descending lithosphere: the effect of varying angle and rate of subduction, Can. J. Earth Sci., 15, 626-641, 1978.
- Talwani, Manik and Maurice Ewing, Rapid computation of gravitational attraction of three-dimensional bodies of arbitrary shape, Geophys., 25, 203-225, 1960.
- Talwani, Manik, George H. Sutton, and J. Lamar Wrozel, A crustal section across the Puerto Rico trench, J. Geophys. Res., 64, 1545-1555, 1959a.
- Talwani, Manik, J. Lamar Wrozel, and Mark Landisman, Rapid computations for two-dimensional bodies with an application to the Mendocino submarine fracture zone, J. Geophys. Res., 64, 49-59, 1959b.
- Talwani, M., J. L. Worzel, and M. Ewing, Gravity anomalies across the Tonga trench, J. Geophys. Res., 66, 1265-1278, 1961.
- Toksoz, M. Nafi and Peter Bird, Formation of marginal basins and continental plateaus, in Island Arcs, Deep Sea Trenches, and Back Arc Basins, Ewing vol. 1, edited by M. Talwani and W. C. Pittman III, pp. 379-393, AGU, 1977.
- Toksoz, M. Nafi, John W. Minnear, and Bruce R. Julian, Temperature field and geophysical effects of a downgoing slab, J. Geophys. Res., 76, 1113-1138, 1971.

- Toksoz, M. Nafi, John W. Minear, and Bruce R. Julian, Temperature field and geophysical effects of a down-going slab, J. Geophys. Res., 76, 1113-1138, 1971.
- Turcotte, D. L. and G. Schubert, Frictional heating of the descending lithosphere, J. Geophys. Res., 78, 5876-5886, 1973.
- Utnasin, V. K., A. I. Abdurakhmanov, G. I. Anosov, Yu. A. Budyansky, V. I. Fedorchenko, Ye. K. Markhinin, and S. T. Balesta Types of magma foci of island arc volcanoes and their study by the method of deep seismic sounding in Kamchatka, in Volcanoes and the Tectosphere, edited by H. Aoki and S. Iizuka, Toaki Univ. Press, Tokyo, pp. 123-137, 1976.
- Watts, A. B. and M. Talwani, Gravity anomalies seaward of deep sea trenches and their tectonic implications, Geophys. J. Roy. Astr. Soc. 36, 57-90, 1974.
- Woollard, G. P., The new gravity system; changes in international gravity base values and anomaly values, in press, 1979.
- Woollard, G. P. and J. C. Rose, International Gravity Measurements, Society of Exploration Geophysicists, Tulsa, Oklahoma, 518, pp., 1963.
- Yoshii, Toshikatsu, Yoshiteru Kono, and Keisuke Ito, Thickening of the oceanic lithosphere, in the Geophysics of the Pacific Ocean Basin and its Margin, Geophys. Mon. Ser., Vol. 19, edited by George H. Sutton, Murli H. Mnagnani, and Ralph Moberly, pp. 423-430, AGU, 1976.

Fig. A4: A comparison of the gravity calculated over the Mariana trough using several different thermal models. The solid line represents the observed free air anomaly and the open circles represent the gravity anomaly calculated using no low density mantle beneath the trough. The x's show the calculated gravity using the model of Schubert et al. (1975) (figure A2) and the +'s are the calculated gravity using Andrews and Sleep (1974) (figure A1). The dots represent the gravity anomaly calculated using the model of Sydora et al. (1978) (figure A3).